Available online at www.sciencedirect.com

SciVerse ScienceDirect

Proceedings of the Combustion Institute 34 (2013) 1569–1576

Proceedings of the Combustion Institute

www.elsevier.com/locate/proci

Spherically symmetric droplet combustion of three and four component miscible mixtures as surrogates for Jet-A

Yu Cheng Liu, Anthony J. Savas, C. Thomas Avedisian *

Sibley School of Mechanical and Aerospace Engineering, Cornell University, Ithaca, NY 14853, USA

Available online 21 June 2012

Abstract

This study examines the droplet combustion characteristics of three and four component miscible liquid mixtures and compares the results with an aviation fuel (Jet-A) burning under the same conditions. The configuration used in the comparison is the base case of spherical symmetry whereby the droplet and flame are spherical and concentric. Mixtures consisting of *n*-decane/*iso*-octane/toluene and *n*-dodecane/*iso*-octane/1,3,5-trimethylbenzene/*n*-propylbenzene in specific molar ratios of 42.67/33.02/24.31 and 40.41/29.48/7.28/22.83, respectively, were previously shown to replicate certain gas phase combustion properties of Jet-A. These specific blends are assessed here for their ability to replicate combustion properties derived from the spherically symmetric case. The data compared include the evolution of the droplet, flame and soot shell diameters. The initial droplet diameter was fixed at 0.56 ± 0.04 mm in the experiments and combustion was carried out in room temperature air under normal atmospheric pressure.

It was found that both blends do replicate certain features of the droplet burning process of Jet-A, though the four component blend performs slightly better. In particular, the sooting propensity and soot standoff ratios are better replicated by the four component blend which is consistent with that blend having been formulated to match the molecular weight and threshold sooting index of Jet-A. Flame standoff ratios and burning rates show a conformance suggested by fuel property variations. The liquid density is identified as a potentially important property in developing liquid surrogate fuels. The results suggest the potential of combustion properties derived from spherically symmetric droplet combustion to assist with developing surrogates for complex transportation fuels.

Keywords: Spherical symmetry; Droplet combustion; Jet-A; Surrogate

1. Introduction

Petroleum-based liquid fuels have powered transportation systems for over a century and demand will be sustained for decades to come [1]. Within the U.S. alone, almost 12 million barrels of oil are consumed per day in ground transportation vehicles which are powered by the internal combustion engine. Sustainable energy produced from wind, solar, geothermal and electric technologies are not yet at the stage where they will significantly impact petroleum use and the emissions they produce (e.g., [2,3]). While these alternatives are being developed to the point where they can

* Corresponding author.
E-mail address: cta2@cornell.edu (C. Thomas Avedisian).

1540-7489/$ - see front matter © 2012 The Combustion Institute. Published by Elsevier Inc. All rights reserved.
http://dx.doi.org/10.1016/j.proci.2012.05.065

Nomenclature

BP	boiling point (K)
$c_{p,g}$	specific heat of gas (J/kg K)
D	droplet diameter (mm)
D_f	flame diameter (mm)
D_o	initial droplet diameter (mm)
D_s	soot shell diameter (mm)
H	height of the ellipse used in image analysis (pixel)
K	burning rate (mm^2/s)
k_g	thermal conductivity of gas (W/m K)
MW	molecular weight (g/mole)
t	time (s)
W	width of the ellipse used in image analysis (pixel)
X_i	liquid mole fraction of species i
Y_i	vapor mole fraction of species i

Greek symbols

v	stoichiometric ratio
ρ_L	liquid density (kg/m^3)

have a significant impact on petroleum consumption and the climate, more immediate benefits can be derived from improving the understanding of the combustion performance of systems powered by conventional liquid fuels. Detailed numerical models of combustion performance in practical devices (e.g., [4,5]) offer significant promise for short term gains by reducing the design cycle for integrating new concepts. However, the complexity of practical fuels limits development of robust predictive tools due to their multi-component nature and variable compositions. Surrogate fuels, defined as blends of relatively fewer compounds of known chemical species and mixture fractions [6–8], that are selected to match certain properties offer the prospect of alleviating this problem.

Real fuels are blends of a wide range of hydrocarbons [9–11]. Figure 1 shows the constituents of the Jet-A blend used in the present investigation. The components identified are consistent with literature observations [7,12–14]. The development of a surrogate that could match selected properties of a fuel like Jet-A is attractive, yet a significant challenge. A simple strategy is to select the constituents to represent broad chemical classes [15] and then to essentially step through a range of compositions of the constituents to identify one that provides a match with the combustion property of interest (e.g., for increments of 0.2 (mole fraction), a binary blend would require stepping through six compositions including the pure components; a three component blend increases the mixture scan to 21 blends including the constituents). A recent study [16] used this approach to identify compositions of heptane/*iso*-octane and heptane/toluene that closely matched the droplet burning characteristics of a commercial grade gasoline. In general, there is no guarantee that a surrogate developed in this way is applicable beyond the specific property the blend was formulated to replicate.

A new approach to developing surrogates was recently proposed [17,18] that is thought to produce a surrogate which is applicable to fuel properties beyond the specific ones used in the development. The approach is rooted in correlating a selected set of fuel properties with distinct molecular fragment groups of the real fuel. Four fuel targets were proposed for determining a larger set of combustion properties if matched with the real fuel: the derived cetane number (DCN); hydrogen-to-carbon (H/C) ratio; threshold sooting index (TSI); and average molecular weight (MW). Each of these properties correlates with a combustion parameter (i.e., DCN with chemical kinetics, H/C with flame temperature, MW with diffusive properties of fuels [19], and TSI with the smoke point of a laminar jet diffusion flame).

A first generation surrogate was developed [17] consisting of *n*-decane, *iso*-octane, and toluene that replicated the H/C ratio and DCN of Jet-A, but which did not match the MW and TSI. The corresponding fractional amounts of the constituents (mole percents) are listed in Table 1. Good agreement was noted with a number of gas phase combustion targets of pre-vaporized (and therefore purely gaseous) fuels. Since the TSI was not

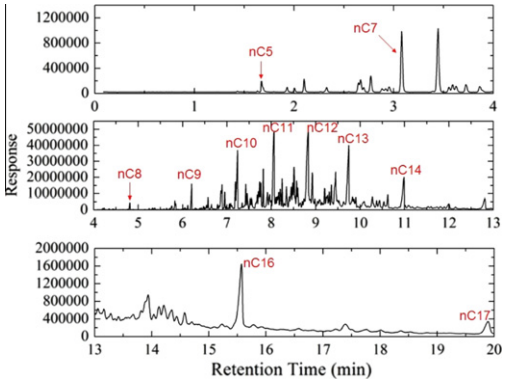

Fig. 1. GC/MS traces of Jet-A (POSF4658).

Table 1
Selected properties of the fuel systems investigated.

Fuel	Pure component	Formula	ρ_L[a] (kg/m^3)	$\rho_{L,mix}$[a] (kg/m^3)	K (mm^2/s)	MW[b] (g/mole)	v	BP[b] (K)	Molar ratio[e]	Volume fraction (%)[f]
	n-Decane	$C_{10}H_{22}$	726			142.28	15.5	447.3	0.4267	50.86
	iso-Octane	C_8H_{18}	688			114.23	12.5	372.4	0.3302	33.34
3CS	Toluene	C_7H_8	862	735	0.62	92.14	9.0	383.8	0.2431	15.80
	n-Dodecane	$C_{12}H_{26}$	745			170.34	18.5	489.5	0.4041	50.36
	iso-Octane	C_8H_{18}	688			114.23	12.5	372.4	0.2948	26.67
4CS	1,3,5-Trimethylbenzene	C_9H_{12}	861	756	0.56	120.19	12.0	437.9	0.0728	5.54
	n-Propylbenzene	C_9H_{12}	858			120.19	12.0	432.4	0.2283	17.43
Jet-A	-	$C_{10.17}H_{19.91}$[c]	800		0.56	142.01[c]	15.1[c]	478-573[d]	-	-

[a] Measured using a digital density meter (Mettler Todelo DA-100M) at 24.6° C.
[b] [27] except for Jet-A.
[c] [17].
[d] [9].
[e] [17,18].
[f] Obtained from listed densities, molecular weights and molar ratios.

matched, the sooting characteristics were not adequately replicated by the three component surrogate (3CS). A later (second generation) four component surrogate (4CS) [18] consisting of *n*-dodecane, *iso*-octane, 1,3,5-trimethylbenzene and *n*-propylbenzene was developed that was able to match all four combustion properties of Jet-A (DCN, H/C ratio, TSI, MW) with the fractional amounts listed in Table 1.

Most of the recent developmental effort for surrogate fuels has concentrated on gas phase combustion characteristics obtained from configurations in which the fuel was completely vaporized before entering the combustion zone (e.g., shock tubes, jet stirred reactors, counter flow diffusion flames, etc.). The fuel vapor composition is thereby known from the initially prepared mixture, as schematically illustrated in Fig. 2a. As transportation fuels are condensed phases (liquids) at operational temperatures the fuel is typically injected into the combustion zone as droplets and sprays. If the flame is sustained by evaporation of the liquid (Fig. 2b) and the liquid is not completely vaporized before ignition, the liquid and vapor compositions will not generally be the same (Fig. 2c).

Combustion targets that arise from burning liquid fuels are as important as those derived from gas phase combustion characteristics. It is not known to what extent surrogates developed to replicate gas phase combustion properties of prevaporized fuels carry over to flames sustained by fuel vaporization. The present study investigates this issue for Jet-A and surrogate blends proposed for it.

An important consideration in the development of surrogate fuels is the selection of a combustion configuration that can provide the targets for the comparison. For liquid fuels, a spray flame is a likely choice, and some early work has used this configuration to assess performance of surrogates for real fuels [20]. However, the flow process of a swirling spray is complex and not easily modeled. The spherical droplet flame is a far more tractable liquid fuel combustion configuration. Figure 3 is a schematic. The flame and droplet are spherical and concentric and soot aggregates are trapped in a shell-like structure by the forces acting on the aggregates (thermophoresis and the flow due to evaporation). This base case of the spherical droplet flame includes some elements in microcosm of more complex (i.e., spray) systems that include evaporation and gas and liquid phase unsteadiness. The idealized configuration of Fig. 3 is used here to assess the extent to which it may serve as a canonical combustion dynamic for developing and testing surrogate fuels.

The fuels examined are Jet-A and the 3CS and 4CS that have been previously reported [17,18]. Table 1 lists representative properties. For the droplet flame the combustion targets of Fig. 3 are the evolution of flame, droplet and soot shell diameters. A question of the present study is the extent to which these variables are predicted by a surrogate developed from gas phase combustion targets that are derived exclusively from prevaporized multi-component fuel blends. In the process, new data are reported for Jet-A for the base case, as well as for miscible fuel blends that incorporate more components than have thus far been examined for the configuration shown in Fig. 3. The compliance with the TSI, in particular, suggests that the 4CS should be better able to match the sooting propensity of Jet-A. Section 2 describes the apparatus and procedures, and Section 3 presents the results.

2. Experimental method

2.1. Setup and procedures

Spherical symmetry in the droplet burning process (or the outer appearance of such) was promoted by using "small" droplets, restricting their movement by anchoring them to very fine diameter support structures, and minimizing the effects of buoyancy by carrying out the experiments in a free-fall facility to reduce gravity and buoyancy effects. The ambient conditions are normal atmospheric pressure and room temperature air. This section briefly discusses the experimental design and procedure. More details are given in [16].

The overall procedure of the experiments is as follows. A piezoelectric generator is used to direct fuel droplets onto two 14 μm SiC fibers, crossed at approximately 60° (Fig. 4a is a planar view), until the droplet reaches the desired size ($D_o = 0.56$ mm). The droplet, generator, electrodes and support fiber mounts (the influence of the support fiber is discussed in [16,21]) are secured in a sealed chamber containing room temperature air at atmospheric pressure. The sealed chamber and cameras are released into free fall for 1.2 s. Gravity levels of about 10^{-4} of Earth's normal gravity are realized during free-fall by placing the instrumentation package inside of a drag shield. Droplet ignition (spark activation) is deliberately delayed to reduce influences of vibration associated with release of the instrumentation package. The sparks are activated 320 ms into the fall and kept on for 800 μs. To reduce spark disturbances, the lowest possible energy that still achieves ignition was employed. The time sequence of package release, spark activation, and electrode retraction is coordinated by a multichannel digital signal generator (Quantum Composer, QC-9618).

The droplet burning process is recorded by two cameras in perpendicular views (Fig. 4b): a color video camera for self-illuminated flame images recorded the evolution of flame shape (Hitachi HV-C20 operated at 30 fps with a Nikkor 135 mm f/2.0 lens and two Kenko 36 mm extension tubes); and a black and white (BW) digital camera with backlighting to record the evolution of droplet and soot shell diameter (a 3.9 MP per frame Canadian Photonics Labs, Inc., MS-80K

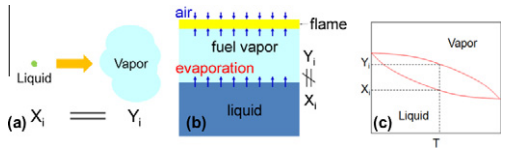

Fig. 2. (a) pre-vaporized fuel parcel of X_i wherein $X_i = Y_i$; (b) flame sustained by evaporation of a liquid mixture of X_i at equilibrium with a gas mixture of Y_i ($X_i \neq Y_i$); (c) phase diagram for a binary mixture.

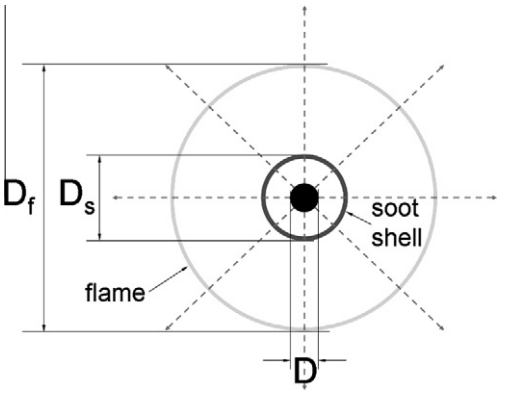

Fig. 3. Idealization of spherical symmetry showing droplet combustion properties. Dotted lines denote streamlines.

digital high speed camera operated at 200 fps, and fitted with an Olympus Zuiko 90 mm f/2.0 lens, an Olympus OM Telescopic Extension Tube 65–116 mm (fixed at 100 mm), and a Vivitar MC 2× teleconverter). Backlighting is provided by a 1 Watt LED lamp (Black Diamond).

Five burning events are examined for each of the fuel blends listed in Table 1. The fuels were obtained from the Sigma–Aldrich Co. in the following purity grades: *n*-decane, 99%; *iso*-octane, 99.8%; toluene, ⩾99.9%; *n*-dodecane, ⩾99%; 1,3,5-trimethylbenzene (mesitylene) ⩾99%; *n*-propylbenzene, 98%. The Jet-A used in this study was supplied by the U.S. Air Force Wright Patterson Air Force Base, with the chemical make-up shown in Fig. 1.

2.2. Image analysis

The images recorded by the BW and color cameras are the main diagnostics of the experiments reported in this paper. The high resolution BW images provide the droplet and the soot shell diameters, while the outer luminous zone diameter of the flame is obtained from the color images.

Figure 5 shows some examples of how the dimensions are extracted from the raw images. A commercial analysis package, Image-Pro Plus v6.3, is used to extract the droplet diameters. An ellipse area of interest (AOI) is applied to the raw BW image to measure the droplet diameter. The red dashed line in Fig. 5a shows the elliptical AOI which is placed on the droplet boundary. The height (H) and width (W) of the ellipse are used to calculate the equivalent diameter by $D = \sqrt{H \times W}$. The alternative image analysis method (a Matlab program developed for automating the droplet size measurements for a series of droplet burning images [22]) is not used for all the analysis in this study owing to the heavily sooting character of the hydrocarbons investigated.

To measure the soot shell diameter an ellipse is manually placed on the shell as shown in Fig. 5b

using the Image-Pro software. A soot shell is considered measureable if there are three or more points which can be identified on the soot shell boundary from which an AOI can be fitted. The flame diameter analyses are developed with the aid of CorelDraw 9. In the present study, the outer boundary of the blue zone which encloses the bright yellow inner core was used as the flame boundary. An elliptical box is placed on the outer boundary of the luminous zone to obtain the flame size as shown in Fig. 5c (dotted line). A 0.79 mm tungsten carbide ball bearing provided a scale factor that is recorded at the same lighting conditions by both cameras.

3. Results and discussion

Evolutions of the flame and soot structures along the combustion history for each fuel investigated in this study are shown in Fig. 6 and Fig. 7, respectively. As shown in Fig. 6, the flame has a yellow inner core with a dimmer faint blue zone at the outer periphery. The yellow inner core is a result of soot incandescence whereas the outer blue zone is indicative of CH emission. The two needle-like glows on the sides of the spherical flame are from the interaction of the flame and the supporting fibers.

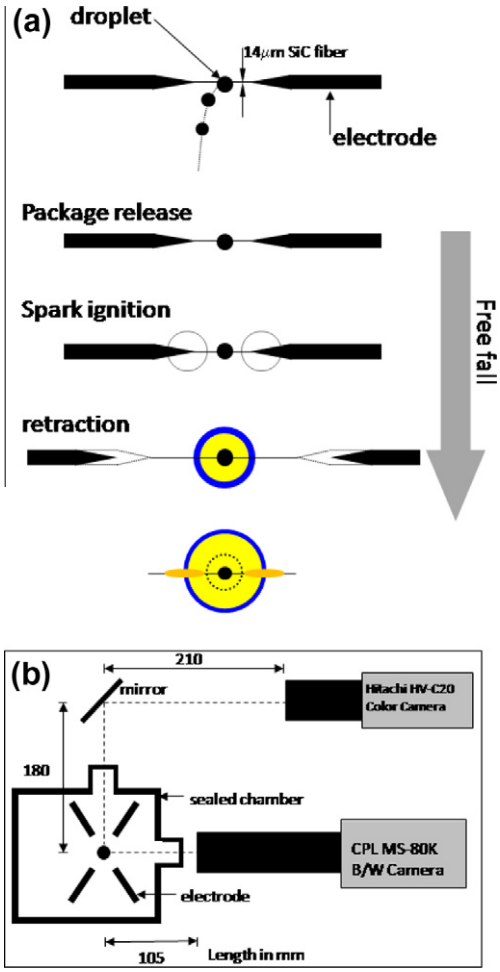

Fig. 4. (a) schematic of procedure; (b) layout of package.

Figure 6 qualitatively shows that Jet-A appears to have the brightest flame among the three fuels. The brightness of the 3CS appears initially to be closer to Jet-A than the 4CS. However, the yellow core of the 3CS seems to diminish faster. A better comparison of the sooting tendencies is shown in Fig. 7 where the soot dynamics are clearly indicated. The soot aggregates form a shell structure 0.1 s after ignition. The 3CS has a less dense soot shell compared to Jet-A or the 4CS. The 4CS soot configuration is (qualitatively) close to Jet-A, which is broadly consistent with this surrogate having matched the TSI of Jet-A [18].

A more quantitative comparison of the surrogates with Jet-A is shown by the evolution of D, D_f and D_s presented in the form of the classical theory of droplet combustion [23], $(D/D_o)^2$, (D_f/D), and (D_s/D) with (t/D_o^2). The evolution of droplet diameter is a macro-scale expression of how the constituents in a fuel droplet are preferentially vaporized (due to the different volatilities of the components) and consumed by the combustion process, and the transient heat transfer associated with the thermal resistances across the liquid and vapor domains. Figure 8 shows the evolution of the droplet size measurements made for the three fuels with the data averaged over five runs for each fuel. Error bars on the averaged Jet-A data show the variation of droplet size measurements between the five runs (the uncertainty of size measurement is much less than the magnitudes of these error bars). Previous measurements for *iso*-octane and toluene [16] are also shown for comparison. The results show that the 4CS is indeed closer to Jet-A than the 3CS. The trend of the *iso*-octane data does not resemble either Jet-A or the 4CS data (nor was it expected to). Toluene is surprisingly close to Jet-A, but it is not suggested that toluene will be a good surrogate for Jet-A overall as it does not replicate other Jet-A targets and its combustion chemistry

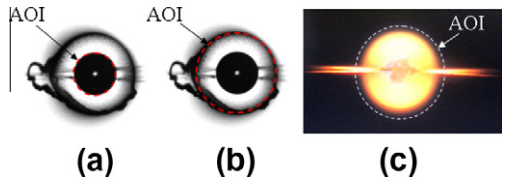

Fig. 5. Illustration of size measurements for (a) a droplet; (b) a soot shell; (c) a flame. The dotted circles (AOIs) are manually placed to determine the dimensions.

is different. This is an indication that a suite of combustion parameters is needed to properly identify an appropriate surrogate for a broader application.

Figure 9 compares the burning rates, $K = -\left(\frac{d(D/D_o)^2}{d(t/D_o^2)}\right)$, calculated from the first derivative of a 4th order polynomial fit of the data shown in Fig. 8. On average, the 3CS burning rates are close to Jet-A, though the 4CS does a slightly better job in the quasi-steady period, $0.6\ \text{s/mm}^2 \le \frac{t}{D_o 2} \le 1.1\ \text{s/mm}^2$. Approximate quasi-steady values from the 4th order fit are listed in Table 1.

The evolutions of flame and soot shell standoff ratios (D_f/D (FSR) and D_s/D (SSR)) are shown in Fig. 10a and b, respectively. The data in Fig. 10a include five individual runs for each fuel as well as averaged data for *iso*-octane and toluene [16]. The FSRs of the surrogates are quite close to Jet-A, with the 3CS higher than Jet-A and the 4CS lower, though the 4CS appears to better match the Jet-A FSR.

The evolution of the SSR is shown in Fig. 10b, which includes five individual runs for each fuel as well as averaged data for *iso*-octane [16]. The lines in Fig. 10b are included to suggest trends. Jet-A and the 4CS appear to have SSRs that follow the same general trends as compared to the 3CS. The 3CS, which does not match Jet-A's TSI, has a larger SSR initially and gradually crosses over Jet-A's SSR. In this respect, not only the sooting propensity of the 4CS is close to Jet-A (cf. Fig. 7) but the transport dynamics of the soot cloud appear to be better matched with the 4CS

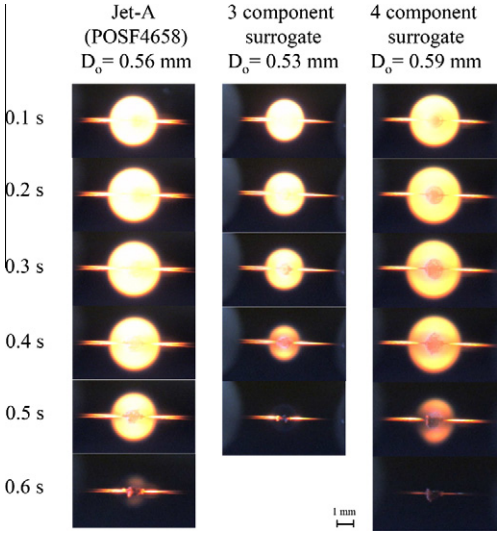

Fig. 6. Color flame images of Jet-A and the 3CS and 4CS examined.

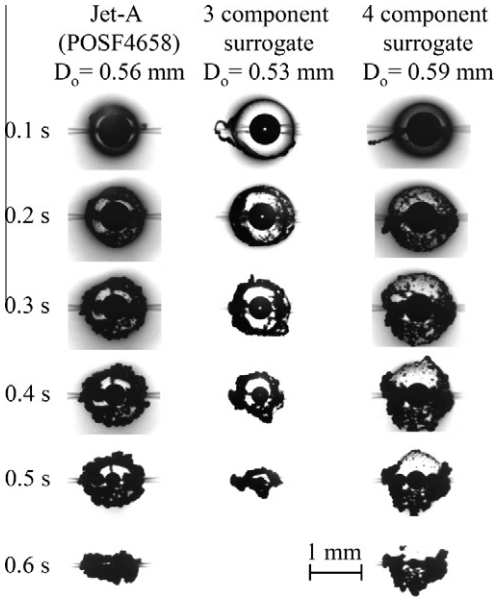

Fig. 7. Black and white images of Jet-A and the 3CS and 4CS examined showing the evolution of the soot shell.

than the 3CS by the consistency of the trends shown in Fig. 10b for Jet-A and the 4CS.

A comprehensive theory of spherically symmetric droplet combustion of sooting fuel blends as complex as those examined here would be useful to further understand the present experimental trends. Work is being pursued along these lines [21,24,25]. Some insights can be gained from the simpler classical theory [23] to identify important properties for developing surrogates that satisfy droplet flame combustion targets. For example, the variation of burning rate shows the importance of the liquid density, gas specific heat, and thermal conductivity, since $K \sim \frac{k_g}{\rho_L c_{pg}}$ with density being a primary control variable. We found that $1.06 < \left(\frac{1/\rho_{L,3,4}}{1/\rho_{L,J}}\right) < 1.08$ using the values in Table 1, which is very close to the comparison for the burning rate (cf. Fig. 9), i.e.,$1.00 < \left(\frac{K_{3,4}}{K_J}\right) < 1.10$. This result suggests that liquid density of a mixture is an important variable for surrogate development which can be added to the suite of combustion parameters (i.e., DCN, H/C ratio, TSI, MW). Similarly, the approximate theory of Aharon and Shaw [26] shows that $\frac{FSR_{3,4}}{FSR_J} \sim \left(\frac{\rho_{L,3,4}}{\rho_{L,J}}\right)\left(\frac{K_{3,4}}{K_J}\right)\left(\frac{\nu_{3,4}}{\nu_J}\right)\left(\frac{MW_J}{MW_{3,4}}\right)$ and liquid density is again seen as important (we found $1.00 < \frac{FSR_{3,4}}{FSR_J} < 1.08$ using property estimates from [27], which is close to $0.98 < \frac{FSR_{3,4}}{FSR_J} < 1.06$ from

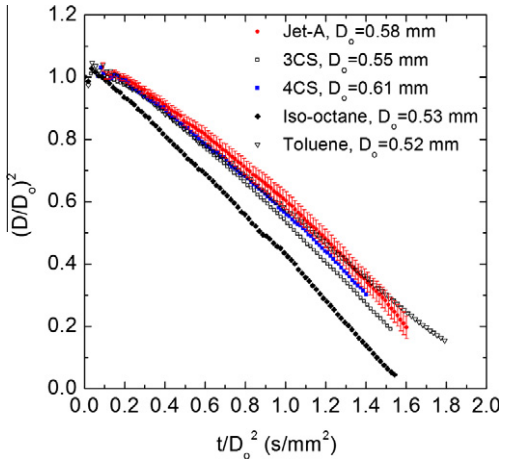

Fig. 8. Evolution of droplet diameters for Jet-A and the 3CS and 4CS (averaged from five individual runs for each of the three fuels). Also shown are data from [16] for *iso*-octane and toluene for comparison.

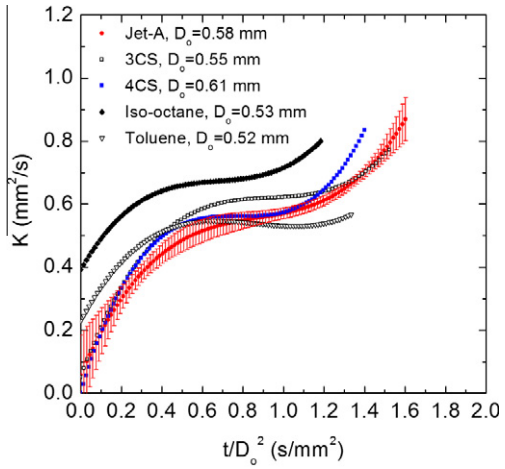

Fig. 9. Burning rates as computed from a 4th order polynomial of the data in Fig. 8.

Fig. 10a, at $t/D_o^2 \sim 0.8$ s/mm^2. By examining the ratios calculated using the values in Table 1, it is found that ρ, K, ν, and MW are equally important to the FSR, though density was not among the targets used to develop these surrogates.

4. Conclusions

Combustion targets derived from the one-dimensional flames of spherically symmetric droplet burning suggest the usefulness of this burning configuration for developing surrogates for real

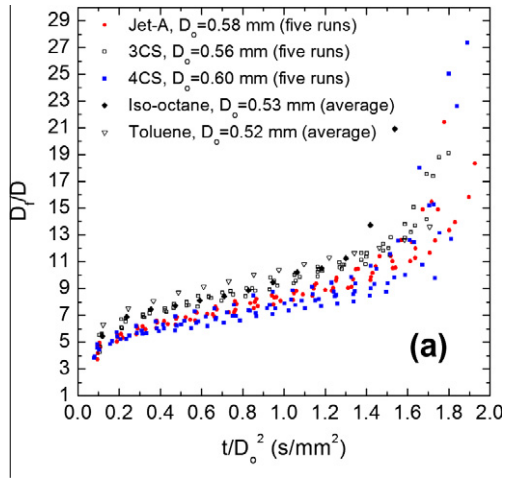

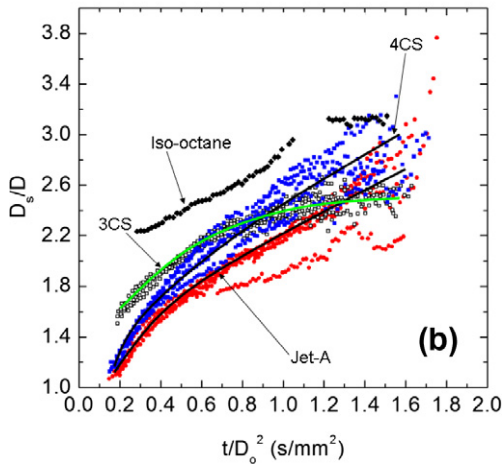

Fig. 10. (a) Evolution of FSR of the fuels investigated comparing to *iso*-octane and toluene [16]; (b) SSR for the fuels investigated comparing with *iso*-octane [16].

fuels. The surrogates examined, which were developed from combustion properties of gaseous (prevaporized) fuels, capture several droplet combustion properties of Jet-A including the evolution of droplet diameter, the flame standoff ratio and qualitative features of the sooting dynamics of Jet-A.

The 4CS showed trends for the SSR more consistent with Jet-A throughout the burning process. This blend also had burning rates close to Jet-A in the quasi-period of burning. The SSR for the 3CS exhibits a different trajectory with time. The FSRs for the three fuels were close to each other, with the 4CS closer to Jet-A than the 3CS. A simple scaling from the classical theory of droplet combustion is consistent with the trends of the experimental results. Overall, the liquid density is considered a relevant target in developing surrogates for complex liquid transportation fuels.

The results also suggest the relevance of the base case for liquid fuel combustion of spherically

symmetric droplet burning as a useful combustion configuration in the development and evaluation of surrogate fuels.

Acknowledgments

The authors thank the National Aeronautics and Space Administration for financial support of this research (Grant Number NNX08AI51G). The authors also thank Mr. Michael Hicks of NASA and Dr. Fred Dryer of Princeton University for helpful discussions. Dr. Tim Edwards of the Wright Patterson Air Force Base provided the Jet-A fuel (POSF4658) for this study and Dr. Xia Zeng of Cornell provided assistance with the GC/MS analysis of Jet-A.

References

[1] "Transforming Combustion Research Through Cyberinfrastructure", Committee on Building Cyberinfrastructure for Combustion Research, National Research Council, The National Academies Press, April 2011 available at (http://nap.edu/catalog.php?record_id=13049), ISBN 978-0-309-16387-3.
[2] R.F. Service, *Science* 319 (2008) 1745.
[3] V. Ramanathan, G. Carmichael, *Nat. Geosci.* 1 (2008) 221–227.
[4] Y. Ra, R.D. Reitz, *Combust. Flame* 158 (2011) 69–90.
[5] Y. Ra, R.D. Reitz, J. McFarlane, C.S. Daw, *SAE Int. J. Fuels Lubr*. 1 (2008) 703–718 (SAE paper no. 2008-01-1379).
[6] H.J. Curran, W.J. Pitz, C.K. Westbrook, C.V. Callahan, F.L. Dryer, *Proc. Combust. Inst.* 27 (1998) 379–387.
[7] T. Edwards, L.Q. Maurice, *J. Propul. Power* 17 (2) (2001) 461–466.
[8] J.A. Cooke, M. Bellucci, M.D. Smooke, et al., *Proc. Combust. Inst.* 30 (2005) 439–446.
[9] M. Colket, T. Edwards, S. Williams, et al., "*Development of an Experimental Database and Kinetic Models for Surrogate Jet Fuels*", *45th AIAA Aerospace Science Meeting and Exhibit*, Reno, Nevada, 2007, AIAA-2007-0770.
[10] J.T. Farrell, N.P. Cernansky, F.L. Dryer, et al., *SAE* 2007-01-0201, 2007.
[11] W.J. Pitz, N.P. Cernansky, F.L. Dryer, et al., *SAE paper* 2007-01-0175, 2007.
[12] B.K. Lavine, H. Mayfield, P.R. Kromann, A. Faruque, *Anal. Chem.* 67 (21) (1995) 3846–3852.
[13] G.L. Hook, G.L. Kimm, T. Hall, P.A. Smith, *Trends Anal. Chem.* 21 (8) (2002) 534–543.
[14] A. Violi, S. Yan, E.G. Eddings, et al., *Combust. Sci. Technol.* 174 (2002) 399–417.
[15] "*Workshop on Combustion Simulation Databases for Real Transportation Fuels*", W. Tsang, J.W. Hudgens, et al., (Eds.), National Institute of Standards and Technology, Gaithersburg, Md., September 4–5, 2003 (NIST report no. NISTIR 7155).
[16] Y.C. Liu, C.T. Avedisian, *Combust. Flame* 159 (2012) 770–783.
[17] S. Dooley, S.H. Won, M. Chaos, et al., *Combust. Flame* 157 (2010) 2333–2339.
[18] S. Dooley, S.H. Won, J. Heyne, et al., *Combust. Flame* 159 (2012) 1444–1466.
[19] A.T. Holley, X.Q. You, E. Dames, H. Wang, F.N. Egolfopoulos, *Proc. Combust. Inst.* 32 (2009) 1157–1163.
[20] R.A. Smith, C.P. Wood, G.S. Samuelsen, AIAA/SAE/ASME/ASEE 21st Joint Propulsion Conference, Monterey, CA, July 8–10, 1985 (AIAA paper no. AIAA-85-1311).
[21] T. Farouk, F.L. Dryer, *Combust. Flame* 159 (2012) 200–209.
[22] C.L. Dembia, Y.C. Liu, C.T. Avedisian, *Image Analysis and Stereology* , 2012, submitted for publication.
[23] S.R. Turns, *An Introduction to Combustion*, second ed., McGraw-Hill Inc, 2006 (Chapter 10) 391.
[24] S. Kumar, A. Ray, S.R. Kale, *Combust. Sci. Technol.* 174 (2002) 67–102.
[25] A.J. Marchese, F.L. Dryer, V. Nayagam, *Combust. Flame* 116 (1999) 432–459.
[26] I. Aharon, B.D. Shaw, *Microgravity Sci. Technol. X-2*, 1997, 75–85.
[27] R.C. Reid, J.M. Prausnitz, T.K. Sherwood, *The Properties of Gases and Liquids*, third ed., McGraw-Hill, New York, 1977.